Yanbu Journal of Engineering and Science

Volume 14 | Issue 1 Article 3

2017

COMPARATIVE STUDY OF CONGO RED ADSORPTION USING DIFFERENT MODIFICATIONS OF RICE STRAW

Ahmad Talaat
Higher Technological Institute, Egypt, ahmadtalaat6363@gmail.com

M. Abdelkreen
Higher Technological Institute, Egypt

Eman Ashour
Minia University, Egypt

Asma Abdelsattar
Minia University, Egypt

Follow this and additional works at: https://yjes.researchcommons.org/yjes

The journal in which this article appears is hosted on Digital Commons, an Elsevier platform.

Recommended Citation

Talaat, Ahmad; Abdelkreen, M.; Ashour, Eman; and Abdelsattar, Asma (2017), COMPARATIVE STUDY OF CONGO RED ADSORPTION USING DIFFERENT MODIFICATIONS OF RICE STRAW, *Yanbu Journal of Engineering and Science*: Vol. 14: Iss. 1, 19-34.
DOI: https://doi.org/10.53370/001c.24328
Available at: https://yjes.researchcommons.org/yjes/vol14/iss1/3

This Research Article is brought to you for free and open access by Yanbu Journal of Engineering and Science. It has been accepted for inclusion in Yanbu Journal of Engineering and Science by an authorized editor of Yanbu Journal of Engineering and Science.

Yanbu Journal of Engineering and Science
ISSN: 1658-5321

Vol. 14, June 2017 (1438H)
www.yjes.org.sa

COMPARATIVE STUDY OF CONGO RED ADSORPTION USING DIFFERENT MODIFICATIONS OF RICE STRAW

Ahmad Talaat[1], M. Abdelkreem[1], Eman Ashour[2], Asma Abdelsattar[2]

[1] Chemical Engineering Department, Higher Technological Institute, 10th of Ramadan City, Egypt
[2] Faculty of Engineering, Chemical Engineering Department, Minia University, Egypt
E-mail: ahmadtalaat6363@gmail.com

ABSTRACT

The aim of this work is to study the removal of Congo red (CR) dye from wastewater using raw rice straw (RRS) and different modifications of it, namely (acid treated rice straw (ATRS), base treated rice straw (BTRS), modified rice straw (MRS) and magnetite loaded rice straw (MLRS)). The effect of contact time, pH, adsorbent dose, mixing rate, particle size and solution temperature on the adsorbed amount of the dye were investigated. The adsorbents were characterized using Fourier transform infrared spectroscopy (FTIR) and scanning electron microscope (SEM). The applicability of Langmuir, Freundlich, Temkin and D-R adsorption isotherm equations for the present system was tested. The experimental data fitted well to Langmuir model for RRS and MLRS and to Freundlich model for other modifications. Kinetic data was analyzed using the pseudo-first-order, pseudo-second-order, Elovich, intra particle diffusion, and film diffusion (Boyd) models and were found to closely follow the pseudo-second-order model. Thermodynamic equations were applied and the results showed that the adsorption was nonspontaneous and exothermic for MRS and spontaneous and endothermic for MLRS.

Keywords: *Adsorption, Congo red, Isotherms, Magnetite, Rice straw.*

1. INTRODUCTION

Synthetic dyes are considered to be harmful organic industrial pollutants. Generally, dyes are used in textiles, dyeing paper, plastics, leather, food industries and cosmetics. The complex aromatic structure of many dyes gives them high stability and makes it difficult to biodegrade [1]. Furthermore, a lot of dyes are highly toxic to several microorganisms and might cause destruction or affect their catalytic capabilities [2]. About 2 % of dyes produced annually are discharged in effluents from many industries [3]. Approximately 20 % of dye production all over the world is lost during dyeing processes and transferred to the aquatic environment [4].

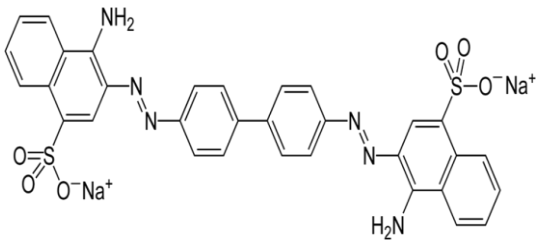

Fig.1. Congo red molecule [5].

Congo red (CR) dye, shown in Figure 1, has a tendency to aggregate inorganic and aqueous solutions. CR color imparts visible

Received: 28 January 2017, Accepted: 10 April 2017

pollution, persistent in streams, decreases the stream reaeration capacity, and affects photosynthetic activity [6]. Several chemical and physical removal techniques have been investigated within the past three decades such as photochemical degradation, coagulation and flocculation [7]. Amongst these techniques, and due to its economical and environmentally friendly reasons, adsorption technique is widely used in wastewater treatment [8]. Adsorption is also quite popular technique because of its simplicity and the availability of many adsorbents. This technique has showed high effectiveness for dye removal [9]. The adsorbents are mainly used without modifications, but in some cases, they undergo some physical and chemical pretreatment processes, such as heating or treatment with chemicals [10]. The pretreatment processes modify the surface groups and their characteristics either by masking the groups, removing them, or by the number of active sites [11]. Researchers used different agricultural wastes as adsorbents for dyes removal [9]. One of these agriculture wastes is rice straw which is used as an adsorbent due to its low cost as well as its high adsorption capacity. About 4.8 million tons of rice are annually produced in Egypt [12]. Rice straw represents 45 % of the volume of rice production [13]. Farmers get rid of rice straw by burning resulting in air pollution. Rice straw is a lignocellulosic agricultural stalk containing lignin (4.9%), silica ash (13.1%), cellulose (37.4%) and hemi-cellulose (44.9%) [14]. Many studies have been reported on CR adsorption using other agricultural wastes such as cattail root, leaf powder, wheat bran, rice bran, rice husk and jute stick powder [7]. Recently, Gong et al [14] prepared modified rice straw with citric acid to get potential adsorbent for dye removal [14]. Chakraborty et al. [15] studied the ability of NaOH-modified rice husk for the removal of crystal violet dye and found an increase in monolayer adsorption capacity [15]. Also, NaOH treatment removes natural waxes and fats from the cellulose fiber surfaces introducing more functional groups [16].

2. MATERIALS AND METHODS

2.1 PREPARATION OF ADSORBENTS

2.1.1 Raw rice straw:

The natural rice straw was washed with distilled water and allowed to dry at 70°C for 8 h. The material was ground and sieved to obtain fractions of different particles sizes.

2.1.2 Rice straw modifications (ATRS, BTRS, MRS and MLRS)

Three samples of RRS (10 g each) was mixed, one with 100 mL (1M) HNO_3 solution to obtain ATRS, the second with 0.75MNaOH solution to obtain BTRS and the third was treated with both the acid and the base in series to obtain MRS. MLRS was prepared by dissolving both $FeCl_3$ and $FeCl_2$ in double distilled water (DDW) with vigorous stirring at 85°C before adding RRS (particle size 75 µm). Then 30% NH_3 solution was added and stirred for 2 h. The material was washed with DDW and 0.02M NaCl and then dried at 50°C for 10 h [17-18]. Many researchers developed different modifications techniques for removal of different contaminants [19].

2.2 ADSORBATE

Congo red (CR), a diazo dye (λ_{max}=500 nm) was obtained from Sigma Aldrich company with chemical formula $C_{33}H_{22}N_6Na_2O_6S_2$, color Index 22120 and MW 696.7 $gmol^{-1}$[20]. Aqueous solutions of the dye with different concentrations were used for calibration.

2.3 ADSORBENT

The complexes on adsorbent surface can be classified as acidic (such as carboxylic, anhydride and lactone groups), basic (such as pyrone and chromene groups), or neutral

(such as carbonyl, quinone and phenolic groups) [16]. The functional groups were characterized by a Fourier transform infrared spectroscopy (FTIR-6100 JASCO) in the range 4000 – 400 cm^{-1}, while the surface morphology was determined by scanning electron microscope (SEM).

3. RESULTS AND DISCUSSION

3.1 CHARACTERIZATION OF THE ADSORBENTS:

3.1.1 Fourier transform infrared spectroscopy (FTIR)

Figure 2a illustrates characteristics of RRS before CR removal. The peak at 3425 cm^{-1} is assigned to stretch O–H groups, the peak 2918 cm^{-1} referred to C–H aliphatic, the peak 1639 cm^{-1} is assigned to C=C stretching and the peak in 1112 cm^{-1} is ascribed to Si-O-Si. After CR removal in Figure 2b, and due to the interaction of the dye molecules and –OH groups on RRS surface some peaks have been changed and others have been created as follow: the peak at 3438 cm^{-1} is assigned to OH stretch water, the peaks 3350 cm^{-1} and 3297cm^{-1} are ascribed to NH stretch (1°, 2° amines, amides), the peak 2861 cm^{-1} indicated the presence of C–H stretch bond and the peak 1042 cm^{-1} referred to C-N stretch bond. This reflects the adsorption of the CR onto RRS. Figure 3a illustrates characteristics of MLRS before CR removal. The peak at 3428 cm^{-1} is assigned to stretch O–H groups and the peak in 551 cm^{-1} is formed which is assigned to Fe_3O_4 on the surface. After CR removal in Figure 3b, some peaks have been created as the peaks at 3260 cm^{-1} and 3315 cm^{-1} referred to NH_2 stretch, the peak at 1031 cm^{-1} referred to C-N stretch bond and the peak in 552 cm^{-1} is ascribed to Fe_3O_4. This reflects the high adsorption of the CR onto MLRS.

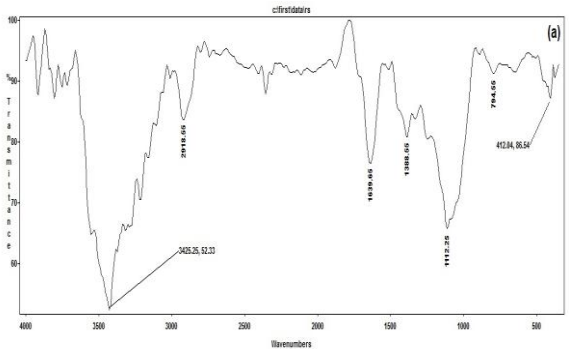

Fig. 2a. FTIR spectrum of RRS before removal

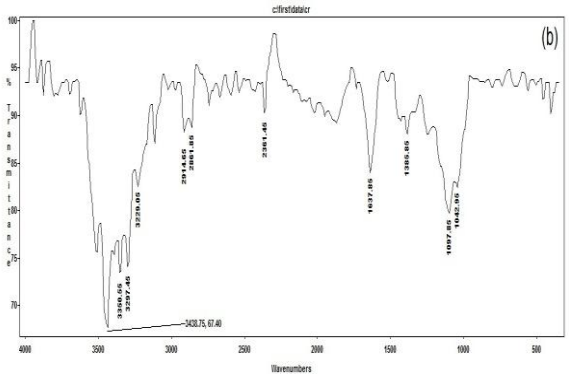

Fig. 2b. FTIR spectrum of RRS after removal

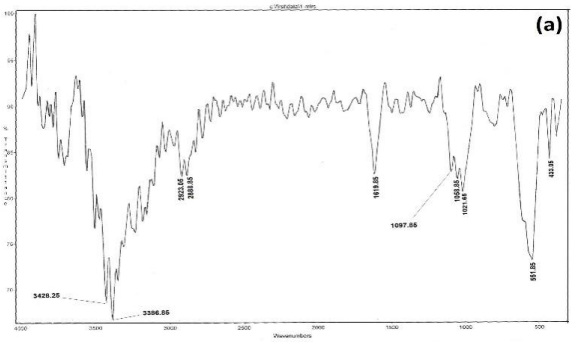

Fig. 3a. FTIR spectrum of MLRS before removal

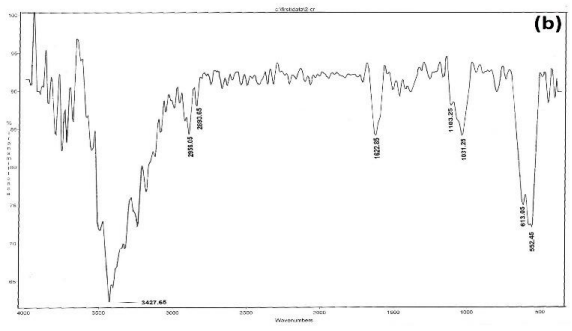

Fig. 3b. FTIR spectrum of MLRS after removal

3.1.2 SCANNING ELECTRON MICROSCOPE (SEM)

Figure 4 indicates the microstructure of the adsorbent particulate before and after modification, and after the dye removal. Before modification large cylindrical units can be observed. Modification of the rice straw has affected its structure. In case of MLRS, the cylindrical units became smaller which increased the surface area. MLRS seems to have higher porous structure with smaller cylindrical unit size compared to the other two adsorbents. On the other hand, MRS cylindrical units have joined together at the walls into a singular solid matrix interspersed with pores probably due to a bridging action occurred after the modification. Still the cylindrical unit size of MRS is less than that of RRS. The figures also shows high filling of the pores by CR in case of MLRS compared with that of RRS. This could reflect the high removal of CR by MLRS.

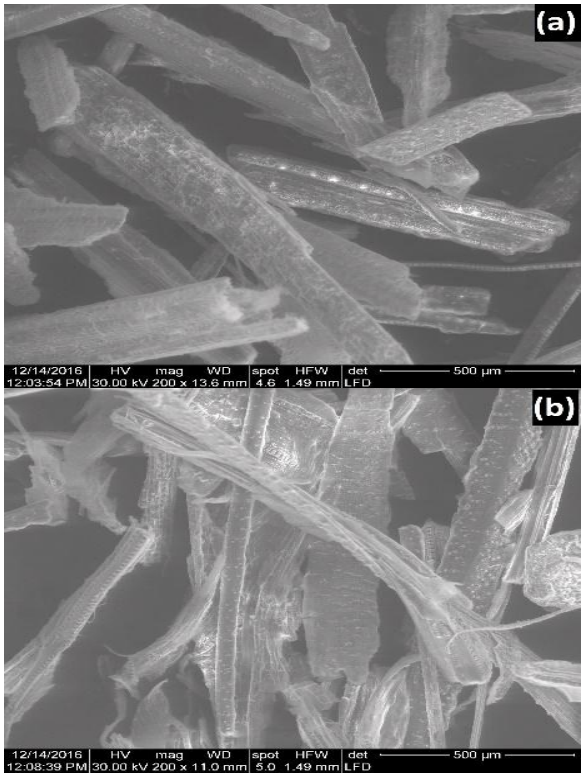

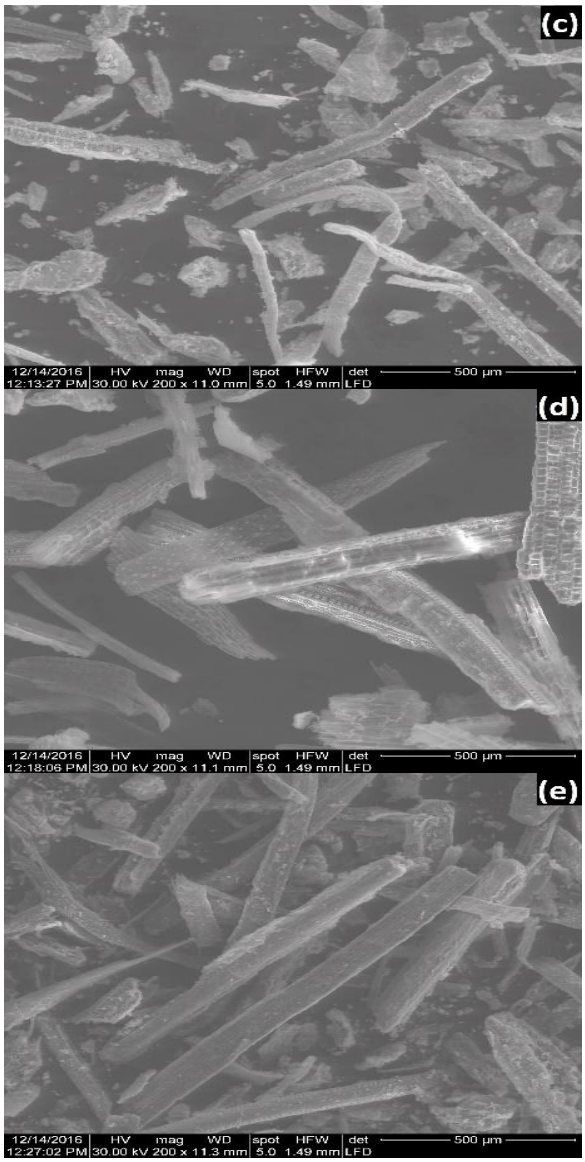

Fig. 4. The SEM image of (a) RRS (b) MRS (c) MLRS (d) adsorbed CR onto RRS (e) adsorbed CR onto MLRS.

3.2 EFFECT OF CONTACT TIME

The dye removal is measured after 5, 10, 15, 30, 60, 45, 90,120, 150, 180 min for initial concentrations 30, 40 and 50 ppm. Figures 5a and 5b depict the adsorption rate of CR onto MRS and MLRS respectively. It can be noticed that the adsorption of dye on the surface of adsorbent follows two different stages. The first stage is a very fast one and can be attributed to the availability of active adsorption sites on the adsorbent surface leading to an increase in driving force due to high concentration gradient [16]. With time,

these sites got occupied and the remaining adsorbate molecules would compete for the remaining unoccupied sites which results in slower adsorption rate representing the second stage. MLRS showed better results which might be attributed to the adsorbent large surface area and good affinity for fast adsorption of dye molecules [21]. Hu et al. found similar results for CR using cattail root [22]. It was observed that equilibrium is reached after 60 min for MRS and 30 min for MLRS.

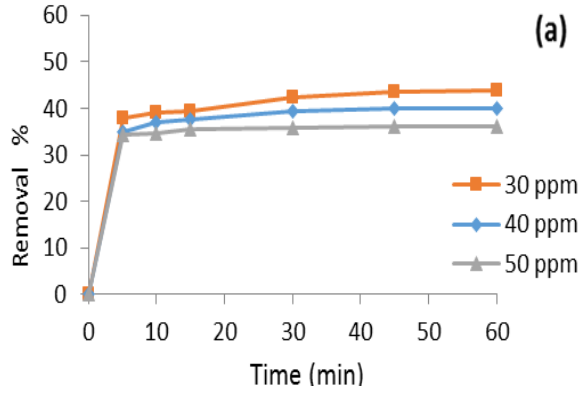

Fig. 5(a). Effect of contact time on the adsorption of CR onto (a) MRS (20 ml solution, adsorbent dose = 0.1g, mixing rate = 100 rpm, particle size = 150 µm, temperature = 25 °C).

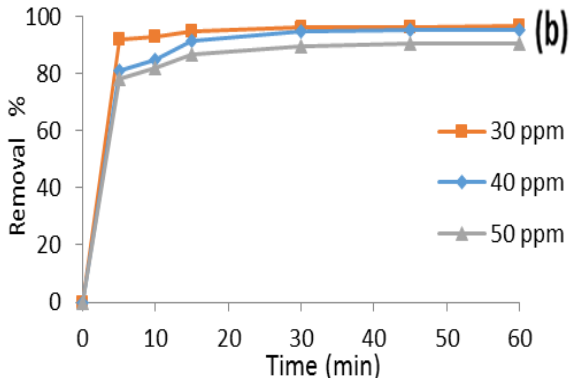

Fig. 5(b). Effect of contact time on the adsorption of CR onto (b) MLRS, (20 ml solution, adsorbent dose = 0.1g, mixing rate = 100 rpm, particle size = 150 µm, temperature = 25 °C).

3.3 Effect of pH

The effect of solution pH on CR removal was investigated and the results were illustrated in Figure 6. The adsorption behavior of MRS was studied at varying pH range of (4-12). The pH of dye solution was adjusted with dilute HCl and NaOH. Varying the initial pH value was found to have a small effect on the adsorbed percent of CR onto MRS which value was varying between 44 and 54 % [21,22]. This may be attributed to the electrostatic interaction between the protonated groups of carbon and acidic dye [23].

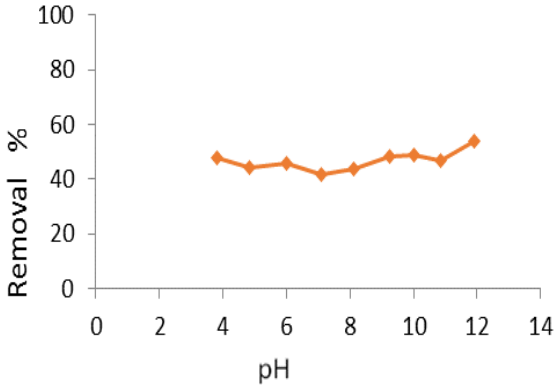

Fig. 6. Effect of initial pH values on the adsorption of CR onto MRS (20 ml solution, time = 60 min, initial dye concentration = 40 ppm, adsorbent dose = 0.1g, mixing rate = 100 rpm, particle size = 150 µm, temperature = 25 °C).

3.4 Effect of Mixing Rate

The effect of mixing rate on the adsorption process for the different tested adsorption systems is illustrated by Figure 7. The dye % removal was investigated vs. degree of agitations at 50, 100, 150, 200, 250 and 300 rpm. It was observed that different mixing rates have a slight effect on CR removal % which changed from 39 to 42 % for MRS and 89 to 93 % for MLRS. This indicates that the adsorption process is not external resistance controlling.

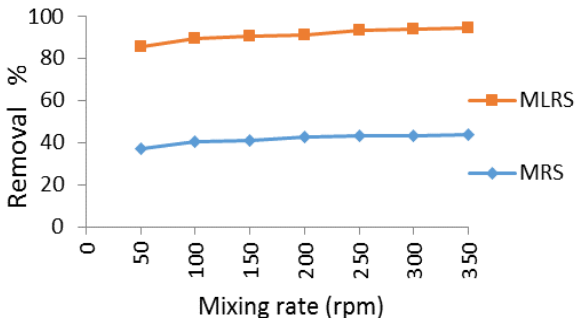

Fig. 7. Effect of degree of agitation on the adsorption of CR onto MRS and MLRS (20 ml solution, time = 60 min for MRS and 30 min for MLRS, initial dye concentration = 40 ppm, adsorbent dose = 0.1g, particle size = 150 µm, temperature = 25 °C).

3.5 Effect of Adsorbent Dose

The effect of adsorbent dosage was studied by varying the adsorbent dosage (0.05-1.5 g) for MRS, RRS and MLRS in 20 ml solution. As shown in Figure 8, the removal % increased from 39 to 97 % for MRS, from 72 to 99 % for RRS and from 83 to 99 % for MLRS. It was observed that almost no extra dye removal beyond 1.4, 0.7, 0.3 gm doses for MRS, RRS and MLRS respectively. This may be due to reaching equilibrium between the adsorbate and adsorbent [20]. The increase in CR removal with the increase of the adsorbent dose is attributed to the surface area increase and hence increasing the vacant sites [24].

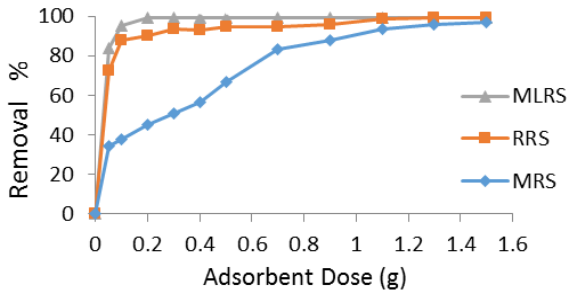

Fig. 8. Effect of adsorbent dose on the adsorption of CR onto MRS and RRS (20 ml solution, time = 60 minfor MRS and RRS and 30 min for MLRS, initial dye concentration = 40 ppm, mixing rate = 100 rpm, particle size = 150 µm, temperature = 25 °C).

3.6 Effect of Particle Size

The effect of particle size on the adsorption removal efficiency was studied in the range of (75, 150, 300 and 600 µm). The data illustrating the relation between particle size and adsorption removal % is depicted by Figure 9. It is clear that there is slight a reduction in dye adsorption associated with increasing in the particle size. The maximum adsorption was obtained at particle size 75 µm. This is due to larger surface area of the adsorbent material that is associated with smaller particle and hence mass transfer resistance decreases [1]. This suggests that the adsorption may be internal resistance controlling.

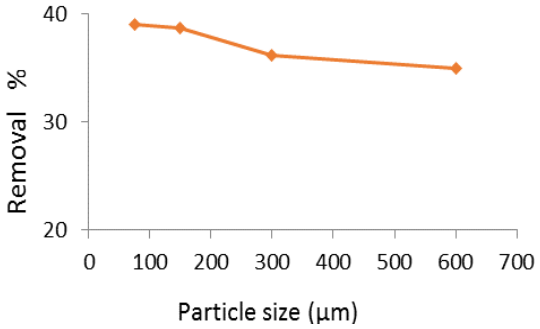

Fig.9. Effect of particle size on the adsorption of CR onto MRS (20 ml solution, time = 60 min, initial dye concentration = 40 ppm, adsorbent dose = 0.1g, mixing rate = 100 rpm, temperature=25 °C).

3.7 Effect of Temperature

Temperature is an indicator for the adsorption nature whether it is an endothermic or exothermic process. The adsorption behavior of MRS and MLRS (shown in Figure 10) was studied at temperatures 25, 40, 55 and 70° C. The results showed that by increasing the temperature, the amount of dye adsorbed increases for MLRS which may be due to the increase in the mobility of the large dye ions with increasing temperature [25]. In contrast, the removal % decreases by increasing the temperature for MRS which may be contributed to the weakening of hydrogen bonds and Van der Walls interaction at higher temperatures, resulting in the weakening of physical interaction between the active sites of the adsorbent and CR molecules [22].

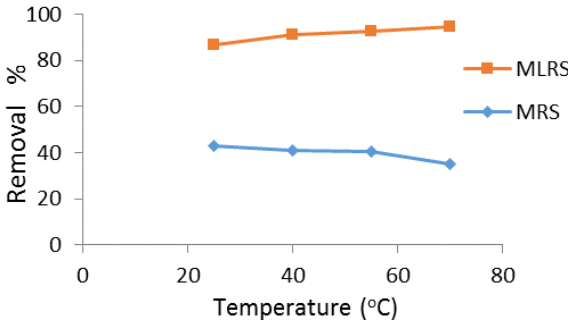

Fig. 10. Effect of temperature on the adsorption of CR onto MRS and MLRS (20 ml solution, time = 60 min, initial dye concentration = 40 ppm, adsorbent dose = 0.1g, mixing rate = 100 rpm, particle size = 150 µm).

Furthermore, increasing adsorption capacity by increasing the temperature indicates that the adsorption process is endothermic. This may be due to the increase in the mobility of the dye molecules and the number of active sites. While decreasing the adsorption capacity with increasing temperature indicates that the adsorption process is an exothermic. In that case, increasing temperature may result in decreasing the adsorptive forces between CR molecules and the active sites on the surface of the adsorbent as a result of decreasing adsorption capacity [26].

3.8 Adsorption thermodynamics

Thermodynamic equations were applied and the values of the constants were obtained from the slope and intercepts as shown in Table 1.The change in standard free energy (ΔG), entropy (ΔS) and enthalpy (ΔH) of adsorption were calculated from the following equations[20]:

$$\Delta G = \Delta H - T\,\Delta S \quad (1)$$

$$\Delta G = R\,T\,\ln Kc \quad (2)$$

$$K_c = C_a/C_e \quad (3)$$

where K_C is the distribution coefficient for adsorption, C_a is the equilibrium dye concentration on the adsorbent (mg L^{-1}) and C_e is the equilibrium dye concentration in solution (mg L^{-1}). ΔH and ΔS of adsorption can be estimated from Van't Hoff equation [23]:

$$\ln K_c = \Delta S/R - \Delta H/RT \quad (4)$$

The slope and intercept of the Van't Hoff equation plot is equal to (-ΔH/R) and (ΔS/R) respectively. For MRS, the positive values of ΔG shows the nonspontaneous nature of adsorption onto MRS. The negative value of ΔH indicates that the adsorption process is exothermic [27]. The negative value ΔS indicates a slight decrease in randomness at the solid-solution interface with increasing temperature and shows the low affinity of the CR towards the adsorbent [22].

TABLE 1: THERMODYNAMIC PARAMETERS OF ADSORPTION OF CR.

MRS

Temp.	ΔG (kJ mol^{-1})	ΔH (kJ mol^{-1})	ΔS ($Jmol^{-1}$ K^{-1})
298	0.64	-5.79	-21.6
313	0.96		
328	1.28		
343	1.61		

MLRS

Temp.	ΔG (kJ mol^{-1})	ΔH (kJ mol^{-1})	ΔS ($Jmol^{-1}$ K^{-1})
298	-4.81	17.47	74.8
313	-5.93		
328	-7.05		
343	-8.17		

For MLRS, the negative values of ΔG indicates the spontaneous nature of the dye adsorption on MLRS as well as the feasibility of the process. With increasing the temperature, ΔG became more negative, indicating that the driving force increased by increasing temperature[27]. The positive values of ΔH indicates that the adsorption process is endothermic [28].The positive values of ΔS suggests an increase in randomness at the solid/solution interface and the high affinity of the CR dye towards the adsorbent [29],[30]. Similar trends for the behavior of CR removal have been reported using coir pith carbon and calcium-rich fly ash [23],[25].

3.9 Adsorption isotherms

The adsorption isotherm describes the interaction mechanism between adsorbate and adsorbent, and shows the adsorption capacity of adsorbent as well. The amount of dye adsorbed is calculated from the following equation[31]:

$$q_e = \frac{(C_o - C_e)V}{m} \quad (5)$$

Where, q_e is the equilibrium adsorbent capacity (mg/g), C_o and C_e are the initial and final dye concentration (mg/L) respectively, V is the volume of the dye solution and m is the mass of the adsorbent (g). The data were

analyzed using Langmuir, Freundlich, Temkin and D-R isotherm models and the values of their corresponding constants were obtained. The isotherms were obtained at an initial CR concentration range of (5–500 mg/L).

3.9.1 Langmuir isotherm

This model describes the formation of a monolayer adsorbate on the adsorbent surface. It assumes uniform energies of adsorption onto the adsorbent surface as well as its homogeneity [20]. The model is represented by the following[10]:

$$\frac{C_e}{q_e} = \frac{1}{q_m K_L} + \frac{C_e}{q_m} \qquad (6)$$

Where C_e is the dye concentration at equilibrium (mg/L), q_e is the adsorption capacity in equilibrium (mg/g), q_m is the maximum adsorption capacity (mg/g), K_L is the Langmuir adsorption constant (L/mg) [32]. The favorability of adsorption can be determined by the dimensionless separation factor (R_L), which is defined by the following equation:

$$R_L = \frac{1}{1 + K_L C_0} \qquad (7)$$

R_L values define whether the adsorption is irreversible ($R_L = 0$), favorable ($0 < R_L < 1$), linear ($R_L = 1$), or unfavorable ($R_L > 1$) [32].

3.9.2 Freundlich isotherm

The Freundlich isotherm is used to describe the adsorption characteristics for heterogeneous surfaces [20]. It can be represented as [33]:

$$\ln q_e = \ln K_f + \frac{1}{n} \ln C_e \qquad (8)$$

where q_e refers to the amount of dye adsorbed per amount of adsorbent at the equilibrium (mg/g), C_e represents the equilibrium concentration (mg/L), and K_f and n are parameters that depend on the adsorbate and adsorbent [34].

3.9.3 Temkin isotherm

This isotherm contains a factor that takes into consideration the adsorbent–adsorbate interactions. By ignoring the extremely low and large value of concentrations. It assumes that heat of adsorption (function of temperature) of all molecules may decrease linearly rather than logarithmic with coverage [35]. The following equation represent Temkin isotherm model [36]:

$$q_e = B \ln A + B \ln C_e \qquad (9)$$

Where A is Temkin isotherm equilibrium binding constant (L/g), B is a constant related to heat of sorption (J/mol), b is Temkin isotherm constant and R is universal gas constant (8.314 J/mol.K).

3.9.4 Dubinin–Radushkevich (DR) isotherm

This isotherm can express the adsorption characteristic onto the adsorbent surface. It is given by the following equation [32]:

$$\ln q_e = \ln q_m - \beta \varepsilon^2 \qquad (10)$$

where, β is a constant related to the mean energy of adsorption (mol^2/kJ^2), q_m is the theoretical adsorption capacity (mg/g), and ε is the Polanyi potential (kJ/mol) and it can be calculated by the followed equation:

$$\varepsilon = RT \ln(1 + 1/C_e) \qquad (11)$$

where R is the gas constant (8.314 J/mol K), T is the absolute temperature (K). The adsorption free energy, E, (J/mol) means the one mole of ions is transferred from the infinity in the solution to the surface of the adsorbent. It can be calculated as [32]:

$$E = \frac{1}{\sqrt{2\beta}} \qquad (12)$$

By comparing the regression coefficient values obtained from Langmuir, Freundlich, Temkin, and D-R isotherm models (presented in Table 2) and fitting the models to the experimental data (depicted by Figures 11 to 13), it can be concluded that Freundlich model effectively fits the experimental data better than other models for ATRS, BTRS

and MRS. Freundlich is an empirical expression that accounts for the surface heterogeneity, exponential distribution of adsorption sites and the sorption energies of these sites. It assumes that adsorption takes place on multilayers on the surface of adsorbent [25]. The value of exponent (n) for all adsorption systems, being greater than 1 shows favorable adsorption condition. Similar trends have been reported for CR adsorption onto modified natural bentonite and coir pith carbon [20]. Langmuir model gives good fit to the experimental data for RRS and MLRS. The maximum adsorption capacities (q_m) increased from 31.19 (mg/g) for RRS to 56.49 and 56.55 (mg/g) for MRS and MLRS respectively. The best fit of equilibrium data in Langmuir isotherm expression confirms monolayer adsorption of CR onto RRS and MLRS adsorbents, as well as the homogeneous distribution of active sites on the surface. The results also demonstrate no interaction and transmigration of CR molecules in the plane of the neighboring surface [37]. The values of R_L were 0.33, 0.75, 0.64, 0.93 and 0.29 for RRS, ATRS, BTRS, MRS and MLRS, respectively. All the calculated R_L values on the different adsorbents were less than 1, which indicates that all systems are favorable. The experimental data showed poor fitting to D-R isotherm model (R^2 between 0.33 and 0.77). However, the mean adsorption energy obtained from this model gives information about the physical or chemical nature of the process. If E<8 kJ/mol, the adsorption is physical, and if 8<E<16, the adsorption is ion exchange, and if E > 16 kJ/mol the adsorption is chemical[32]. Since E values are between 0.2 and 5.7 (kJ/mol) (less than 8) then the adsorption has a physical nature.

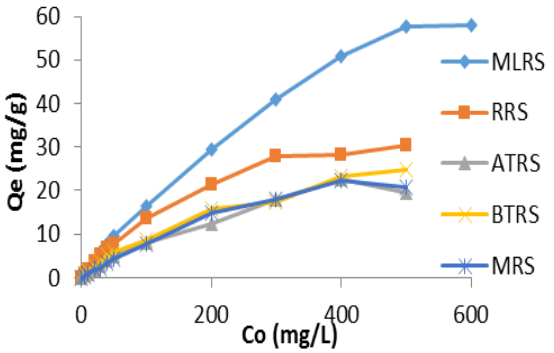

Fig. 11. Adsorption isotherm for CR dye using different modifications of RS.

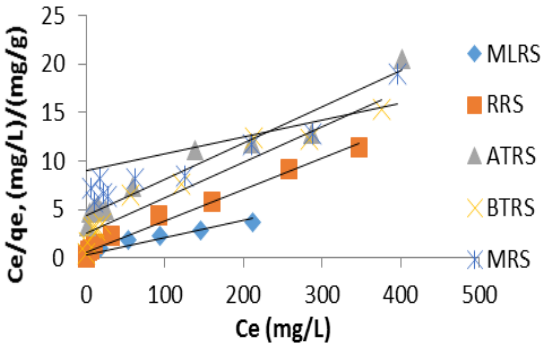

Fig. 12. Langmuir isotherm for CR dye using different modifications of RS.

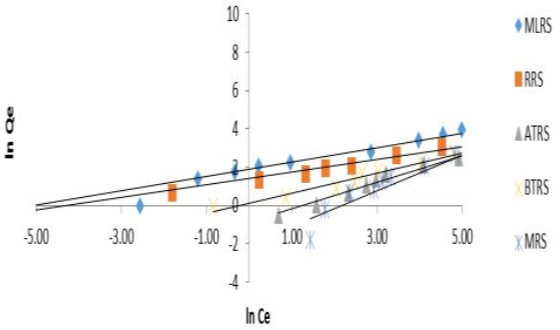

Fig. 13. Freundlich isotherm for CR dye using different modifications of RS.

TABLE 2: ADSORPTION ISOTHERMS PARAMETERS FOR CR ADSORPTION.

Isotherms	Parameter	Different modifications of RS				
		RRS	ATRS	BTRS	MRS	MLRS
Freundlich	R^2	0.976	0.980	0.982	0.910	0.912
	n	3.004	1.440	1.921	1.076	2.670
	K_f	4.166	0.418	1.125	0.135	6.704
Langmuir	R^2	0.986	0.955	0.936	0.150	0.942
	q_{max}	31.192	26.859	27.353	56.490	56.551
	K_L	0.050	0.008	0.014	0.002	0.063
	R_L	0.33	0.75	0.64	0.93	0.29
Temkin	R^2	0.755	0.887	0.822	0.924	0.769
	B	2.910	4.327	3.743	5.207	5.278
	A	12.600	0.206	0.537	0.132	14.175
	b	851.4	572.5	661.9	475.8	469.4
D-R	R^2	0.459	0.481	0.374	0.776	0.339
	K_{DR}	0.015	2.803	0.259	15.057	0.015
	X_m	11.019	7.125	7.780	8.687	14.724
	E	5.7	0.4	1.4	0.2	5.7

3.10 KINETICS STUDIES

The kinetic of the adsorption describes the reaction pathway along times until reaching equilibrium. It also helps in defining the sorption efficiency [38].In the present work, adsorption kinetics has been evaluated using five kinetic models: pseudo-first-order, pseudo-second order equations, Elovich, intraparticle diffusion, and film diffusion(Boyd) models. A pseudo-first-order kinetic equation is given as [39]:

$$\ln (q_e - q_t) = \ln q_e - k_1 t \qquad (13)$$

The pseudo second-order kinetic is given as[40]:

$$(t/q_t) = (1/k_2 q_e^2) + (t/q_e) \qquad (14)$$

where, k_1 is the pseudo-first-order rate constant (1/min), k_2 is the pseudo second order rate constant of adsorption (g/mg min), q_t and q_e are the amount of dye adsorbed at time t and at equilibrium (mg/g), respectively. A simplified linearized form of Elovich kinetic equation is presented as follows [41]:

$$q_t = (1/\beta) \ln(\alpha\beta) + (1/\beta) \ln(t) \qquad (15)$$

where, α is the initial adsorption rate (mg/g min) and β desorption constant (g/mg). The plot of q_t against ln t provides a linear relationship from which α and β are determined as the slope and intercept of the plot. An intraparticle diffusion model is given as [42]:

$$q_t = k_{id}\, t^{0.5} + C \qquad (16)$$

where, q_t is the amount of solute on the surface of the sorbent at time t (mg/g), k_{id} is the intraparticle diffusion rate constant (mg/g $min^{0.5}$) and C is the intercept. All the experimental data (Figure 14 and Table 3), showed better fitting with pseudo second-order kinetic model which appeared in the high regression coefficient (R^2) values for the entire concentration range. Therefore, it can be concluded that the rate of dyes adsorption is influenced by the interaction between the dye molecules and the functional groups distributed on the adsorbent surface [11]. Such result is obtained because pseudo second order describes data related to adsorption on heterogeneous and/or porous systems or energetically homogeneous adsorbents [43]. The pseudo-first-order model data is not appropriate since it didn't give straight lines for most of the initial concentrations [7]. The prediction of the rate determining mechanism affects the adsorption system design. The adsorption process in an aqueous solution is characterized by either external mass or intraparticle diffusion or both. The inapplicability of intra-particle diffusion model (Figure 15) reveals that the intra-particle diffusion is not the only step controlling the adsorption process. If the intra-particle diffusion was the only step

that controls the adsorption, then a plot of the amount of the adsorbate adsorbed per unit mass of adsorbent (q_t) against square root of time ($t^{0.5}$) would give a straight line passing through the origin [20]. If the line does not pass through the origin, other mechanism may be involved. In this case, the intercept gives an indication about the thickness of the boundary layer [44]. The effect of the boundary layer increases by increasing the intercept. Else it is understood that the boundary layer diffusion may be controlling the adsorption [7]. The kinetic data was further analyzed by Boyd's film-diffusion model to identify the film resistance role. This model assumes that the boundary layer surrounding the adsorbent particle is the main resistance to diffusion, and can be calculated by the following equation [44]:

$$B_t = -0.4977 - (\ln (1 - F)) \quad (17)$$

where, B_t is the mathematical function of F and F represents the fraction of solute adsorbed at time t (h) and $F = q_t / q_e$. The calculated B_t values were plotted against time that is used to identify whether film diffusion or intra-particle diffusion controls the rate of mass transfer. If the plot of B_t versus time is linear and pass through the origin, the adsorption rate is governed by film diffusion model; otherwise, it is controlled by intra-particle diffusion. The plot of CR adsorbed by various adsorbents does not pass through the origin, indicating the film diffusion was not only the rate determining step [44]. The Elovich model can be used in describing adsorption on heterogeneous surfaces. However, it does not predict any mechanism. The poor fitting of data to Elovich model shows the physical nature of the adsorption process which support the results obtained from D-R isotherm [45].

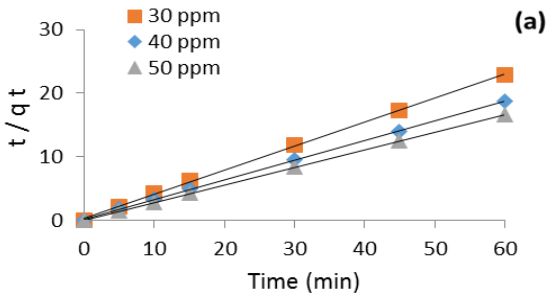

Fig. 14(a). Pseudo-second order kinetic model for CR dye, Co = (30, 40, 50) ppm MRS.

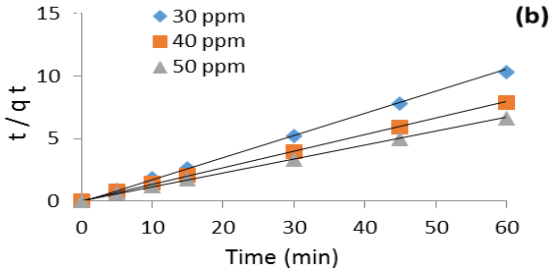

Fig. 14(b). Pseudo-second order kinetic model for CR dye, Co = (30, 40, 50) ppm MLRS.

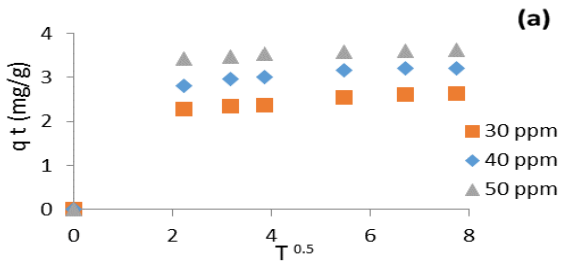

Fig. 15(a). Intraparticle diffusion model for CR dye, Co = (30, 40, 50) ppm MRS.

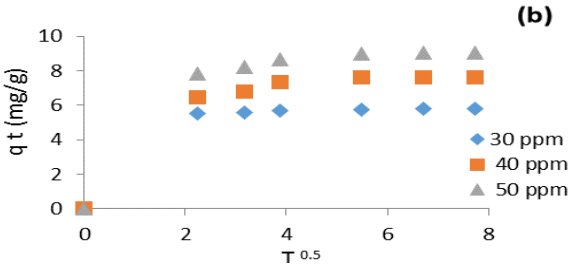

Fig. 15(b). Intraparticle diffusion model for CR dye, Co = (30, 40, 50) ppm MLRS.

TABLE 3: KINETIC PARAMETERS FOR ADSORPTION OF CR.

Models	Parameter	Different modifications of RS						
		RRS (40ppm)	MRS (30ppm)	MRS (40ppm)	MRS (50ppm)	MLRS (30ppm)	MLRS (40ppm)	MLRS (50ppm)
Pseudo-first-order	R^2	0.919	0.893	0.909	0.782	0.812	0.955	0.919
	k_1	0.098	0.094	0.106	0.105	0.112	0.134	0.113
	q_e	3.084	1.089	1.207	0.698	1.179	3.477	3.433
Pseudo-second-order	R^2	0.999	1.000	1.000	1.000	1.000	1.000	1.000
	k_2	0.062	0.258	0.303	0.677	0.433	0.116	0.108
	q_e	7.550	2.680	3.261	3.635	5.838	7.803	9.234
Intra particle	R^2	0.539	0.610	0.590	0.519	0.519	0.615	0.598
	k_{id}	0.485	0.273	0.333	0.360	0.578	0.811	0.950
	C	3.435	0.966	1.228	1.532	2.461	2.824	3.435
Elovich	R^2	0.957	0.957	0.976	0.963	0.953	0.910	0.938
	β	2.060	6.611	5.963	12.72	7.956	2.003	1.925

4. CONCLUSION

The results showed that the rice straw is suitable and low cost adsorbent for removing CR dye especially when loaded with magnetite. The experimental work indicated that pH value has a small effect on the uptake of CR dye. The equilibrium concentration was found at 60 and 30 min for MRS and MLRS respectively. The experimental results were best fitted to Langmuir isotherm model for RRS and MLRS, and Freundlich isotherm model for ATRS, BTRS and MRS. The recommended particle size is 75 μm. The isotherm constants show the physical nature of the adsorption process. The kinetics of adsorption of CR has been correlated to pseudo-second order coefficient. The obtained values of thermodynamic parameters indicate that the adsorption process is nonspontaneous and exothermic in nature for MRS adsorbent and spontaneous and endothermic for MLRS. These results reveal that rice straw could be used as adsorbent for dye removal from contaminated water and can be recommended for wastewater treatment plants.

ACKNOWLEDGEMENTS

The author would like to thank the Chemical Engineering Department members at the British University in Egypt (BUE) for their great support.

REFERENCES

[1] A. Mittal, J. Mittal, A. Malviya, and V. K. Gupta, "Adsorptive removal of hazardous anionic dye 'Congo red' from wastewater using waste materials and recovery by desorption," J. Colloid Interface Sci., vol. 340, no. 1, pp. 16–26, 2009.

[2] R. Ansari and Z. Mosayebzadeh, "Removal of basic dye methylene blue from aqueous aolutions using sawdust and saedust coated with polypirrole," J. Iran. Chem. Soc., vol. 7, no. 2, pp. 339–350, 2010.

[3] K. S. Bharathi and S. T. Ramesh, "Removal of dyes using agricultural waste as low-cost adsorbents: a review," Appl. Water Sci., vol. 3, no. 4, pp. 773–790, 2013.

[4] S. Boumaza, F. Kaouah, S. Omeiri, M. Trari, and Z. Bendjama, "Removal of dyes by an integrated process coupling adsorption and photocatalysis in batch mode," Res. Chem. Intermed., vol. 41, no. 4, pp. 2353–2375, 2015.

[5] H. Patel and R. T. Vashi, "Removal of Congo red dye from its aqueous solution using natural coagulants," J. Saudi Chem. Soc., vol. 16, no. 2, pp. 131–136, 2012.

[6] C. N. N.Kanchana, "Removal of Congo red from aqueous solution by waste banana pith," Pertanika J. Sci. Technol., vol. 1, no. 1, pp. 33–42, 1993.

[7] M. C. Somasekhara Reddy, L. Sivaramakrishna, and A. Varada Reddy, "The use of an agricultural waste material, jujuba seeds for the removal of anionic dye (Congo red) from aqueous medium," J. Hazard. Mater., vol. 203–204, pp. 118–127, 2012.

[8] R. V. Rousseau, Handbook of separation process technology, 1st ed. 1987.

[9] B. Zhao, Y. Shang, W. Xiao, C. Dou, and R. Han, "Adsorption of Congo red from solution using cationic surfactant modified wheat straw in column model," J. Environ. Chem. Eng., vol. 2, no. 1, pp. 40–45, 2014.

[10] E Worch, Adsorption technology in water treatment, 2nd ed. 2012.

[11] Z. Yaneva and N. Georgieva, "Insights into Congo red adsorption on agro-industrial materials - spectral, equilibrium, kinetic, thermodynamic, dynamic and desorption studies. A Review," Int. Rev. Chem. Eng., vol. 4, no. 2, pp. 127–146, 2012.

[12] T. Badawi, "Rice research accomplishment in Egypt," Ciheam, vol. 15, no. 3, pp. 105–116, 1997.

[13] C. G. Rocha, D. A. M. Zaia, R. V. da S. Alfaya, and A. A. da S. Alfaya, "Use of rice straw as biosorbent for removal of Cu(II), Zn(II), Cd(II) and Hg(II) ions in industrial effluents," J. Hazard. Mater., vol. 166, no. 1, pp. 383–388, 2009.

[14] R. Gong, Y. Jin, F. Chen, J. Chen, and Z. Liu, "Enhanced malachite green removal from aqueous solution by citric acid modified rice straw," J. Hazard. Mater., vol. 137, no. 2, pp. 865–870, 2006.

[15] S. Chakraborty, S. Chowdhury, and P. Das Saha, "Adsorption of crystal violet from aqueous solution onto NaOH-modified rice husk," Carbohydr. Polym., vol. 86, no. 4, pp. 1533–1541, 2011.

[16] N. a. Fathy, O. I. El-Shafey, and L. B. Khalil, "Effectiveness of alkali-acid treatment in enhancement the adsorption capacity for rice straw: The removal of methylene blue dye," ISRN Phys. Chem., pp. 1–15, 2013.

[17] T. Madrakian, A. Afkhami, and M. Ahmadi, "Adsorption and kinetic studies of seven different organic dyes onto magnetite nanoparticles loaded tea waste and removal of them from wastewater samples," Spectrochim. Acta - Part A Mol. Biomol. Spectrosc., vol. 99, pp. 102–109, 2012.

[18] Sameh S. H. Haridi, A. A. Zekry, M. A. Radwan, and M. A. Sharaf, "Evaluation and Characterization of Magnetic Carboxymethyl Chitosan Nanocomposite for Removal of Zink and Lead from Waste-water," J. Am. Sci., vol. 8, no. 11, pp. 38–43, 2012.

[19] A. Talaat, M.Abdelkreem, E. Ashour, and A. Abdelsattar, "Comparative study of methylene blue adsorption using (raw, acid, base, modified, magnetite loaded) rice straw," J. Int. Acad. Res. Multidiscip., vol. 4, no. 8, pp. 29–47, 2016.

[20] B. J. Manjot Toor, "Adsorption characteristics, isotherm, kinetics, and diffusion of modified natural bentonite for removing diazo dye," Chem. Eng. J., vol. 187, pp. 79–88, 2012.

[21] T. Madrakian and A. Afkhami, "Adsorption of some cationic and anionic dyes on magnetite nanoparticles-modified activated carbon from aqueous solutions: Equilibrium and kinetics study," J. Iran. Chem. Soc., vol. 10, pp. 481–489, 2013.

[22] Z. Hu, H. Chen, F. Ji, and S. Yuan, "Removal of Congo red from aqueous solution by cattail root," J. Hazard. Mater., vol. 173, no. 1–3, pp. 292–297, 2010.

[23] C. Namasivayam and D. Kavitha, "Removal of Congo red from water by adsorption onto activated carbon prepared from coir pith, an agricultural solid waste," Dye. Pigment., vol. 54, no. 1, pp. 47–58, 2002.

[24] K. A. Tan, N. Morad, T. T. Teng, I. Norli, and P. Panneerselvam, "Removal of cationic dye by magnetic nanoparticle (Fe3O4) impregnated onto activated maize cob powder and kinetic study of dye waste adsorption," APCBEE Procedia, vol. 1, pp. 83–89, 2012.

[25] B. Acemioğlu, "Adsorption of Congo red from aqueous solution onto calcium-rich fly ash," J. Colloid Interface Sci., vol. 274, no. 2, pp. 371–379, 2004.

[26] M. A. M. Salleh, D. K. Mahmoud, W. A. W. A. Karim, and A. Idris, "Cationic and anionic dye adsorption by agricultural solid wastes: A comprehensive review," Desalination, vol. 280, pp. 1–13, 2011.

[27] S. Chowdhury and P. Saha, "Sea shell powder as a new adsorbent to remove basic green 4 (malachite green) from aqueous solutions: Equilibrium, kinetic and thermodynamic studies," Chem. Eng. J., vol. 164, no. 1, pp. 168–177, 2010.

[28] S. Chowdhury and P. Das Saha, "Biosorption of methylene blue from aqueous solutions by a waste biomaterial: hen feathers," Appl. Water Sci., vol. 2, no. 3, pp. 209–219, 2012.

[29] Y. A. Akl MA, "Solid phase extraction and spectrophotometric determination of methylene blue in environmental samples using bentonite

and acid activated bentonite from Egypt," J. Anal. Bioanal. Tech., vol. 05, no. 01, pp. 1–8, 2014.

[30] M. R. Malekbala, M. A. Khan, S. Hosseini, L. C. Abdullah, and T. S. Y. Choong, "Adsorption/desorption of cationic dye on surfactant modified mesoporous carbon coated monolith: Equilibrium, kinetic and thermodynamic studies," J. Ind. Eng. Chem., vol. 21, pp. 369–377, 2015.

[31] R. A. Rezk, A. H. Galmed, M. Abdelkreem, N. A. A. Ghany, and M. A. Harith, "Quantitative analysis of Cu and Co adsorbed on fish bones via laser-induced breakdown spectroscopy," Opt. Laser Technol., vol. 83, pp. 131–139, 2016.

[32] L. Yu and Y. M. Luo, "The adsorption mechanism of anionic and cationic dyes by Jerusalem artichoke stalk-based mesoporous activated carbon," J. Environ. Chem. Eng., vol. 2, no. 1, pp. 220–229, 2014.

[33] M. Suzuk, Adsorption engineering, 1st ed. 1990.

[34] M. B. Desta, "Batch sorption experiments: Langmuir and Freundlich isotherm studies for the adsorption of textile metal ions onto teff straw (eragrostis tef) agricultural waste," J. Thermodyn., pp. 1–6, 2013.

[35] A. . Dada, A. . Olalekan, A. . Olatunya, and O. Dada, "Langmuir , Freundlich , Temkin and Dubinin – Radushkevich isotherms studies of equilibrium sorption of Zn 2 + unto phosphoric acid modified rice husk," IOSR J. Appl. Chem., vol. 3, no. 1, pp. 38–45, 2012.

[36] R. Wu et al., "Hydrothermal preparation of magnetic Fe3O4@C nanoparticles for dye adsorption," J. Environ. Chem. Eng., vol. 2, no. 2, pp. 907–913, 2014.

[37] V. . Copello, G.J., Diaz, L.E. and Dall' Orto, "Adsorption of Cd(II) and Pb(II) onto a one step-synthesized polyampholyte: Kinetics and equilibrium studies," J. Hazard. Mater., vol. 2, pp. 374–381, 2012.

[38] M. H. and P. M. D. Prasath, "Adsorption of malachite green onto carbon prepared from borassus bark," Arab. J. Sci. Eng., vol. 34, no. 2a, pp. 31–42, 2009.

[39] D. Robati, "Pseudo-second-order kinetic equations for modeling adsorption systems for removal of lead ions using multi-walled carbon nanotube," J. Nanostructure Chem., vol. 3, no. 1, pp. 1–6, 2013.

[40] A. K. Kushwaha, N. Gupta, and M. C. Chattopadhyaya, "Removal of cationic methylene blue and malachite green dyes from aqueous solution by waste materials of daucus carota," J. Saudi Chem. Soc., vol. 18, no. 3, pp. 200–207, 2014.

[41] Y. Li et al., "Comparative study of methylene blue dye adsorption onto activated carbon, graphene oxide, and carbon nanotubes," Chem. Eng. Res. Des., vol. 91, no. 2, pp. 361–368, 2013.

[42] N. A. Oladoja, C. O. Aboluwoye, and Y. B. Oladimeji, "Kinetics and isotherm studies on methylene blue adsorption onto ground palm kernel coat," Turkish J. Eng. Environ. Sci., vol. 32, no. 5, pp. 303–312, 2008.

[43] D. S. Anna Derylo-Marczewska, Katarzyna Miroslaw AdamW. Marczewski, "Studies of adsorption equilibria and kinetics of microporous carbons ...," Adsorption, vol. 16, pp. 459–375, 2010.

[44] S. N. A. S. A. B. Mandal, "Adsorption isotherms , kinetics and mechanism for the adsorption of cationic and anionic dyes onto carbonaceous particles prepared from Juglans regia shell biomass," Int. J. Environ. Sci. Technol., vol. 10, pp. 231–242, 2013.

[45] R.-S. J. Feng-ChinWua, Ru-Ling Tsengb, "Characteristics of elovich equation used for the analysis of adsorption kinetics in dye – chitosan systems," Chem. Eng. J., vol. 2, pp. 366–373, 2009.

دراسة مقارنة لإمتزاز صبغه أحمر الكونغو باستخدام معالجات مختلفة من قش الأرز

أحمد طلعت[1]، محمد عبد الكريم[2]،إيمان عاشور[2]،أسماء عبد الستار[2]

[1] قسم الهندسة الكيميائية، المعهد التكنولوجي العالي، مدينة العاشر من رمضان، مصر

[2] كليه الهندسة، قسم الهندسة الكيميائية، جامعة المنيا، مصر

الملخص:

يهدف البحث إلى دراسة إزالة صبغة أحمر الكونغو من المحاليل باستخدام قش الأرز الخام (RRS) وتعديلات مختلفة منه: قش الأرز المعالج بالحامض (ATRS), قش الأرز المعالج بالقلوي (BTRS), قش الأرز المعدل (MRS) وقش الأرز الحامل لخواص مغناطيسية (MLRS). تم دراسة تأثير زمن التعرض ودرجة الحموضة وكتلة المادة المازة ومعدل التقليب ومقاس حبيبات الممتز ودرجة الحرارة على الكمية الممتزة من الصبغة. وقد تم دراسة المادة الممتزة بالأشعة تحت الحمراء FTIR والمايكروسكوب الإلكتروني الماسح لمحاولة تفسير النتائج. وتم تحليل النتائج المعملية لعملية الاتزان باستخدام النماذج الرياضية: "لانجماير" و"فروندليش" و"دى آر وتيمكن"، وتبين من الدراسة أن النتائج المعملية تتوافق إلى حد كبير مع نموذج "لانجماير" لقش الأرز الخام وقش الأرز الحامل لخواص مغناطيسية بينما يتماشى نموذج "فروندليش" مع باقي التعديلات المختلفة من قش الأرز. كما تم تحليل نتائج كيناتيكية الامتزاز باستخدام النماذج الرياضية: نموذج تفاعل الدرجة الأولى pseudo-first-order, ونموذج تفاعل الدرجة الثانية pseudo-second-order, والانتشار الداخلي للجسيمات intraparticle diffusion, إيلوفيتش Elovich و بويد Boyd. وقد وجد أن نموذج تفاعل الدرجة الثانية هو الأكثر قدرة على تمثيل النتائج. وتم إيجاد المتغيرات الحرارية لعملية الامتزاز وأوضحت النتائج أن عملية الامتزاز غير تلقائية وطاردة للحرارة لقش الأرز المعدل, و تلقائية وماصة للحرارة لقش الأرز الحامل لخواص مغناطيسية.